*J. Synchrotron Rad.* (1999). **6**, 852–864

# Structure of metal centres in proteins at subatomic resolution

**S. Samar Hasnain[a] and Keith O. Hodgson[b]**

*[a]CLRC Daresbury Laboratory, Warrington WA4 4AD, UK, and [b]Stanford Synchrotron Radiation Laboratory, SLAC, California, USA*

(*Received 29 March 1999; accepted 14 May 1999*)

Metalloproteins perform a wide variety of biological functions and, in doing so, in many cases exploit the redox properties and the coordination chemistry of the metal atom. The structural changes associated with the different coordination and redox changes can be quite small and can only be visualized at a very high resolution. The advent of synchrotron radiation has provided the possibility of studying these proteins by X-ray crystallography at 'atomic' resolutions. Synchrotron radiation has also revolutionized another X-ray technique, XAFS (X-ray absorption fine structure), where modulations in atomic absorption take place due to the scattering of photo-excited electrons from the immediate surrounding of the photon-absorbing atom. The dependency of XAFS on synchrotron radiation is even more acute than protein crystallography, as a continuous X-ray spectrum of high intensity is required for the experiment. In fact, the source and monochomator requirements are very similar for XAFS and MAD (multiple-wavelength anamolous diffraction). The local nature of the XAFS has advantages in that no crystalline order is required and that the resolution is the same in the aqueous, amorphous or crystalline system, *i.e.* subatomic resolutions are intrinsically present in the data. This review, written in recognition of Sir John Walker's Nobel prize, for which synchrotron radiation played a key role, also provides some recent case studies to illustrate the advantages of this technique and its synergy with the synchrotron-based crystallography.

**Keywords: metalloproteins; superoxide dismutase; molybdenum enzymes; cupredoxins; MAD; EXAFS.**

## 1. Introduction

XAFS† provides very high (subatomic‡) resolution information about a specific centre such as the metal atom in a metalloprotein. In fact, the resolution of XAFS can be essentially the same for small molecules and large metalloproteins. Despite the very high resolution of the technique and its equal applicability to crystalline and aqueous state, its full power is achieved only when it is combined with the three-dimensional high-resolution structure, generally available from X-ray crystallography. This three-dimensional structure may be of the protein under study itself or of a closely related system. The purpose of this review is to provide an overview of the XAFS technique and highlight some aspects of its development and applications to selected metalloproteins. The usefulness of this *combined approach* for structure–function studies of metalloproteins will be demonstrated through some recent examples. We hope to demonstrate that the combination of a very high resolution crystallographic study of the metalloproteins in the resting state and the atomic/subatomic resolution XAFS of resting and reactive intermediate states is a very powerful approach for studying structure–function relationships in these important (and colourful) proteins.

### 1.1. *Metalloproteins and crystallography*

Metalloproteins form a large fraction (between a quarter and a third) of all known proteins. These contain metal ions either as a single atom or as part of a cluster and play a variety of life-sustaining roles in the bacterial, plant and animal kingdoms (Harrison, 1985). In the list of 25 elements that have been recognized as essential and indispensable to life, 15 are metals. Some of the fundamental biological processes in which metalloproteins participate include electron storage and transfer, dioxygen binding, storage and activation, and substrate transport, catalysis and activation. In addition to their abundance and importance in the biosphere, many of the metalloproteins are coloured due to metal–ligand charge-transfer bands. The colour of these biologically important molecules not only make them aesthetically attractive but also offers much practical advantage in biochemical manipulation. Thus, it is not surprising that these proteins have attracted much attention from biophysicists including some of the

† XAFS is used when the whole of the X-ray absorption spectrum is referred; EXAFS when the extended region above the edge is referred; XANES when structure near the absorption edge is referred.

‡ Use of the term subatomic resolution is made to distinguish it from the term atomic resolution; atomic resolution is defined as 1.2 Å where C—C bonds are visible; subatomic refers to a resolution where redox states can be distinguished, *i.e.* where the effects of an individual electron with respect to the metal centre can be defined.

**Table 1**
Highest resolution X-ray structures of *some* metalloproteins.

For each protein class, the total number of structures in PDB (as of 1 April 1999) are given. Structures of mutant proteins are not included. Some of the papers remain unpublished but reference date is given as it appears in the PDB.

| PDB ref. | Protein | Author | MW (kDa) | Resolution (Å) |
|---|---|---|---|---|
| Rubredoxins (17 Structures) | | | | |
| 1RB9 | Rubredoxin | Dauter *et al.* (unpublished) | 6 | 0.92 |
| 1BRF | Rubredoxin (WT) | Bau *et al.* (1998) | 6 | 0.95 |
| 1IRO | Rubredoxin | Dauter *et al.* (1996) | 6 | 1.10 |
| 4RXN | Rubredoxin (unconstrained) | Watenpaugh *et al.* (1980) | 6 | 1.20 |
| 5RXN | Rubredoxin (constrained) | Watenpaugh *et al.* (1980) | 6 | 1.20 |
| Ferredoxins (65 Structures) | | | | |
| 2FDN | 4Fe-4S Ferredoxin | Dauter, Wilson *et al.* (1997) | 13 | 0.94 |
| 7FD1 | 7-Fe Ferredoxin | Stout *et al.* (1998) | 13 | 1.30 |
| Cytochromes (226 structures) | | | | |
| 1C52 | Cytochrome-C552 | Than *et al.* (1997) | 14.2 | 1.28 |
| 1CTJ | Cytochrome C6 | Frazao *et al.* (1995) | | 1.10 |
| 1YCC | Cytochrome C (Isozyme 1) | Louie & Brayer (1990) | 12.7 | 1.23 |
| Myoglobins (146 structures) | | | | |
| 1A6G | Carbonmonoxy-myoglobin | Chu *et al.* (1998) | 17.8 | 1.15 |
| 1BZ6 | Aquomet myoglobin | Kachalova *et al.* (1999) | 17.8 | 1.20 |
| Concanavalin A (29 structures) | | | | |
| 1NLS | Concanavalin A | Deacon *et al.* (1997) | 25 | 0.94 |
| 1JBC | Concanavalin A | Parkin *et al.* (1996) | 25 | 1.20 |
| Calcium binding protein (150 structures) | | | | |
| 2PVB | Pike parvalbumin | Declerq *et al.* (1999) | 12 | 0.91 |
| 1psr.pdb | Human psoriasin (S100*a*7) | Brodersen *et al.* (1998) | 11.7 | 1.05 |
| 1b9o.pdb | α-Lactalbumin | Harata *et al.* (1999) | 14.2 | 1.15 |

pioneers (Dorothy Hodgkins, Perutz, Kendrew, Phillips) of protein crystallography (*e.g.* see Kendrew *et al.*, 1958; Perutz, 1970).

Metalloproteins utilize the chemistry of metals to their advantage to perform varied biological functions with specification and control. The redox and ligand chemistry of metals is used to perform a wide variety of chemical reactions in the biosphere. Quite often, these chemical reactions are accompanied by only a small structural change around the metal atom. Thus, ideally, atomic-resolution structures of these proteins are required in different reaction states, but a knowledge of the very high resolution structure of the metal centre in itself is of major benefit for understanding the chemistry/reaction mechanisms of metalloenzymes. It perhaps is fair to claim that nowhere in the determination of molecular structure is precision more at a premium than in the case of metalloproteins. It is thus understandable why high-resolution (<2 Å) structure determination of metalloproteins has attracted so much attention (see *e.g.* Dauter, Lamzin *et al.*, 1997). In many cases, it has not been possible to obtain atomic-resolution (<1.2 Å, where individual atoms become visible) crystallographic data due to inherent diffraction limits of protein crystals arising from the static disorder or other factors. Table 1 provides a list of some of the highest resolution crystal structures of metalloproteins (see Tables 3 and 4 also). It is clear that only a handful of structures are known to atomic resolutions; the largest being Concanavalin A, with a molecular weight of 25 kDa, which is known to 0.94 Å and is one of the highest resolution structures to date (Deacon *et al.*, 1997).

### 1.2. *XAFS*

Soon after the first X-ray experiment using X-rays from a synchrotron for muscle diffraction (Rosenbaum *et al.*, 1971), the Krönig and Kössel structures of the physics textbooks were transformed into a ubiquitous technique called XAFS (X-ray absorption fine structure) (Sayers *et al.*, 1971; Kincaid & Eisenberger, 1975; Lytle, 1999), which found immediate applications in biology, chemistry, geology and material science (see *e.g.* Cramer & Hodgson, 1979; Goulon *et al.*, 1997). The growth of the subject has been very rapid and can be judged by the size of the proceedings for the first international XAFS conference (140 typed pages) held in March 1981 at Daresbury (Garner & Hasnain, 1981) and the tenth conference held in August 1998 in Chicago (over 700 printed pages of the *Journal of Synchrotron Radiation*, May 1999 issue). Worldwide, the number of XAFS instruments continue to increase; some 25% of all synchrotron radiation instruments are either devoted or partially used for XAFS. These instruments are generally located in close proximity to protein crystallography stations and thus opportunities of intellectual exchange as well as technology transfer exist. This is clearly seen in Fig. 1, which shows a layout of the SRS. We note, for historical interest, that the size of

experimental hutches have increased into full-size rooms with the emergence of dedicated storage rings. Fig. 2, in contrast, shows a view of the world's first EXAFS 'hutch' on SSRL beamline 1–5.

XAFS arises primarily from the scattering of ejected photoelectrons and is a final-state effect. It can thus be pictured as an electron diffraction experiment where the source of the electron is the photo-excited metal centre and

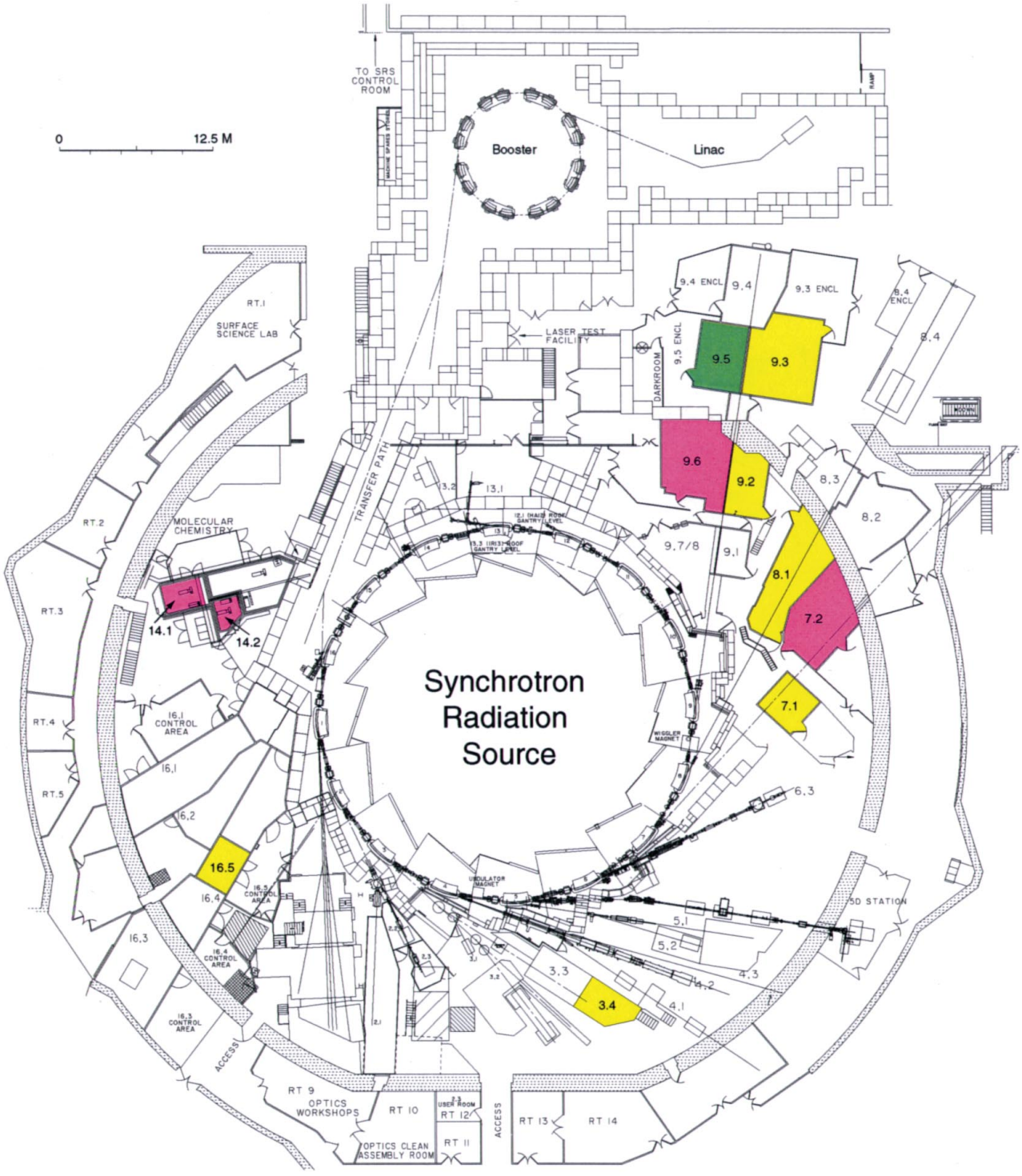


**Figure 1**
As an example, a layout of the Synchrotron Radiation Source (SRS) is given indicating the XAFS stations (hutches) in yellow, 'slow tunable' PX stations in magenta and a 'fully tuneable' MAD station in green. The two multipole wiggler PX stations (14.1 and 14.2) soon to come on-line are indicated by arrows. Station 14.2 is optimized for work at the selenium edge (0.93 Å). [For details of the PX stations and their development at SRS, see Cassetta *et al.* (1999) in this issue.]

the diffracted electron's detector is also the same metal centre. Surface scientists use a technique called LEED (low energy electron diffraction) routinely for probing the structure of surfaces where diffraction of low-energy electrons from a surface is used for structure determination (Pendry, 1974). Thus, it is not surprising that the theory of XAFS is based on electron scattering (Ashley & Doniach, 1975; Lee & Pendry, 1975). The pathlength of electrons (mean free path) for most of the XAFS range (electron energy > 50 eV) is such that single-scattering events dominate the extended range. Near the absorption edge, *i.e.* for electron energies < 50 eV, many multiple-scattering paths exist and the data interpretation still requires a heroic effort (Binsted & Hasnain, 1996). These two regions of XAFS are referred to as EXAFS (extended X-ray absorption fine structure) and XANES (X-ray absorption near-edge structure). In addition to the electron-scattering effects, the near-edge part of the XANES spectrum contains electronic structure information and can sometimes be interpreted in terms of bound-state transitions. Even a qualitative comparison of this region is powerful in providing information about the redox state of the metal centre. Even though the EXAFS region is generally dominated by single-scattering events, strong multiple-scattering events can exist for much of the EXAFS region. This is the case for protein ligands such as histidine and tyrosine, groups such as pyroles and for ligands/substrates/inhibitors such as CO, NO, CN *etc.* or special arrangements of multinuclear metal centres (Co *et al.*, 1983; Blackburn *et al.*, 1987; Strange *et al.*, 1987; Hasnain & Strange, 1990). The multiple scattering is strongest when two atoms are collinear with the metal atom and sharply drops off as the angle reduces from 180° with little contribution at angles less than 110°. These multiple-scattering effects can be treated in data analysis if proper care is taken and offer the opportunity for extracting angular information between the scattering centres (see *e.g.* Zhang *et al.*, 1996, 1997).

XAFS is applicable equally to both the aqueous and crystalline state (Bianconi *et al.*, 1985), even though the majority of applications have been to the aqueous proteins. In a number of cases, data have been obtained on a crystalline slurry (Ascone *et al.*, 1997) though there are examples of applications to protein single crystals (Scott *et al.*, 1982). One of the primary reasons for the lack of XAFS data on single crystals is the lack of suitable instruments [some MAD (multiwavelength anomalous diffraction) instruments are capable of this] where high-quality fluorescence data from single crystals (<100 μm) can be obtained. However, even these are not equipped with the best of fluorescence detectors making reliable EXAFS measurements extremely time-consuming.

## 2. Theoretical advances

An approximate formulation of the EXAFS theory was worked out during the mid-1970s by Stern (1974) and developed extensively by Lee & Pendry (1975) and Ashley & Doniach (1975). During the next 20 years many other contributions to the development of EXAFS theory occurred (Gurman *et al.*, 1984, 1986; Foulis *et al.*, 1990; Muster de Leon *et al.*, 1990; Pettifer *et al.*, 1986; Rehr *et al.*, 1994, Filipponi *et al.*, 1995). It has been shown that, in general, except for the energies very close to the absorption threshold, a single-scattering formalism is sufficient to describe the observed data in most cases (Lee & Pendry, 1975; Ashley & Doniach, 1975). Initially, multiple-scattering contributions were not considered to be important in the EXAFS region, except for a collinear arrangement of scattering atoms. However, it was noted by several workers (see *e.g.* Blackburn *et al.*, 1984; Pettifer *et al.*, 1986) that, in the case of imidazole ligands, strong multiple-scattering contributions are present in the EXAFS up to 300 eV above the absorption edge. Perutz *et al.* (1982) had pointed out that if such contributions could be analysed, then stereochemical details such as the position of the Fe atom with respect to the haem plane can be determined. These multiple-scattering contributions mainly arise due to backscattering from the distal (outer shell) atoms of imidazole/pyrole groups, where the photoelectron is forward scattered by the intervening N atom before being backscattered by the outer-shell atom. Forward scattering is generally strong at lower electron energies ($E$ < 200 eV) over a significant angular range (0–70°). At higher electron energies the strong forward scattering is increasingly confined to a narrower cone and the multiple-scattering

**Figure 2**
The world's first EXAFS 'hutch' on SSRL beamline 1–5. The first hard X-ray EXAFS spectra using synchrotron radiation were recorded in this hutch including the first EXAFS of proteins (Myoglobin). The first fluorescence EXAFS was performed by 'poking' a hole in the side of the hutch and sticking in the snout of a detector.

**Table 2**
Some early XAFS studies carried out in the first five years (1975–1980) which have stood the test of time.

| Year | Authors† | Main results |
|---|---|---|
| 1975 | R. G. Schulman, P. Eisenberger, W. E. Blumberg, N. A. Stombaugh | EXAFS of rubredoxin showed that the four Fe—S distances were equal in length, in contrast to the then available crystal structure results |
| 1978 | S. P. Cramer, K. O. Hodgson, W. O. Gillum, L. E. Mortenson | The first application of EXAFS to determine *de novo* a metal site in a metalloprotein was the remarkable discovery of an unprecedented polynuclear Mo–Fe–S cluster in the nitrogenase enzyme from the EXAFS data analysis |
| 1978 | S. P. Cramer, J. H. Dawson, K. O. Hodgson, L. P. Hager | Applications to cytochrome P-450 quantified the presence of an axial sulfur ligand |
| 1978 | T. D. Tullius, P. Frank, K. O. Hodgson | The 'blue copper protein' azurin was found to have an unusually short Cu—S ligand which defined the electronic structure of the active site |
| 1979, 1980 | J. Bordas, R. C. Bray, C. D. Garner, S. Gutteridge, S. S. Hasnain | First difference EXAFS to show that functional form of xanthine oxidase contained a cyanosable sulfur (essential for catalysis) at the Mo site |

† See References for details.

contributions become unimportant except when an approximately collinear geometry exists. The higher-order scattering terms become even more important in the X-ray absorption near-edge region. Multiple scattering of the excited electron provides the possibility of obtaining information about bond angles, relative orientations of metal ligands and thus a fuller stereochemical picture of the metal site in a protein. This region of the spectrum has also become tractable to theoretical interpretation and offers a unique method of obtaining a higher correlation function in aqueous protein samples (see *e.g.* Durham *et al.*, 1981; Bianconi *et al.*, 1985; Joly, 1997).

It is obviously highly desirable to be able to utilize the whole XAFS region in structural studies and much effort has been made towards a unified analysis approach for the two regions. A comparison of matrix inversion and finite path sum methods shows that the later method is more promising for fitting the edge region. Recent developments have made the calculations of both the scattering and atomic components practicable and thus have made the fitting of an entire X-ray spectrum rather than its components, EXAFS and XANES, possible (Binsted & Hasnain, 1996). However, a number of improvements are still required before this approach can be used for 'routine' structure determination.

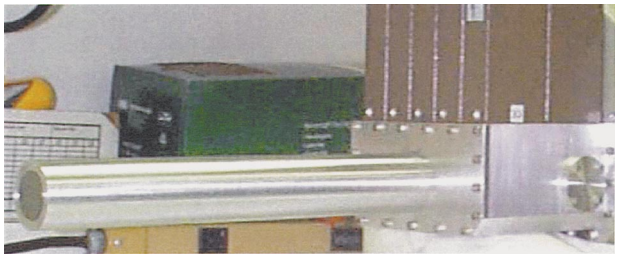

**Figure 3**
A picture of a low-profile nine-element solid-state fluorescence detector. The low profile of the detector makes it adaptable on a single-crystal diffractometer.

Much of the early work was based on the 'plane-wave approximation'. More recently, much effort has been put towards the use of *exact* methods. The curved-wave approach based on 'Lee and Pendry's' formalism has been long used for structural studies of metalloproteins (Bordas *et al.*, 1980; Strange *et al.*, 1987; Blackburn *et al.*, 1987; Murphy *et al.*, 1993, 1997; Liu *et al.*, 1994; Shiro *et al.*, 1997; Baugh *et al.*, 1997). These exact methods have been combined with restrained and constrained refinement approaches in order to utilize the known stereochemical (bond distances and angles within a group) information and maintain a reasonable ratio of parameters to observations (Binsted *et al.*, 1992). There are now several widely recognized packages available, which are based on 'exact' theory, *e.g. EXCURV*, *FEFF*, *GNXAS*, and their availability to the wider community is likely to improve the quality of structural information.

## 3. Experimental advances for XAFS and their impact on PX

A synchrotron source is a prerequisite for protein XAFS, thus, to date, there has been no XAFS study of a metalloprotein using a laboratory X-ray source. In addition to the source, the relatively low metal (absorbing atom) concentration of ~0.5–5 mM puts extreme demands on fluorescence detectors, which developed early on as the primary means of studying dilute metalloproteins (Jaklevic *et al.*, 1977). In fact, it is the application of XAFS to proteins which has driven the development of multi-element detection systems based on Ge/Si (Li) detector technology (Cramer *et al.*, 1988; Derbyshire *et al.*, 1999) with parallel development in purpose-built front-end electronics (Derbyshire *et al.*, 1992). In addition, a complete tunability of wavelength with high resolution ($\Delta\lambda/\lambda \simeq 10^{-4}$) is required to record the near-edge and extended fine structure, thus necessitating the use of a double-crystal monochromator (Kincaid & Eisenberger, 1975). Again, it is

the application to dilute systems, including proteins, which has prompted the rapid scanning of these monochromators without compromising the wavelength stability or spectral purity (Frahm, 1989; Murphy *et al.*, 1995). Thus, it is now practical to sweep the whole of the XAFS spectrum within a matter of seconds. The source and monochromator requirements of single-crystal XAFS are very similar to those of a MAD beamline. Indeed, the two crystal scanning monchromator systems developed for early XAFS instruments are now routinely used on most dedicated MAD beamlines. The alignment requirements of the sample are also the same. The fluorescence detector for single-crystal applications needs to be somewhat special given the small sample volume and limited access to the sample due to the diffractometer, cryostream *etc*. Recently, a low-profile nine-element detector (C-TRAIN), Fig. 3, has been developed for fluorescence XAFS applications (Derbyshire *et al.*, 1999) with the requirement that it can be fitted around complex sample stages such as those encountered in crystallographic data collection. The nose cone of the detector is very similar in dimensions to the current cryostreams, which are in use at most crystallographic set-ups. Both of these developments, namely a rapidly scanning monochromator and an energy-dispesive low-profile solid-state detector, are likely to prove important for MAD beamlines as well as single-crystal XAFS studies.

## 4. Applications

XAFS has been applied to a large number of metalloproteins over the last 20 or so years. It is worth remarking that several of the pioneering studies have stood the test of time; some of these are summarized in Table 2.

### 4.1. *Electronic information*

4.1.1. *K-edge XANES*. Two types of information can be obtained from this region. As has been said before, this region is sensitive to the electronic configuration of the metal site, thus changes in the redox state of the metal or in its stereochemistry causes changes in the spectrum in this region. Such edge transitions can be especially useful in providing quantitative insight into electronic structure. This information can be particularly important in the investigation of high-valence metals as constituents of oxidants, reactive intermediates, and materials with interesting conductive and magnetic properties. High-energy (*i.e.* X-ray) spectroscopies have played an important role in identifying and describing the bonding character of high-valence metals in such materials (Hu *et al.*, 1998). As a specific example relevant to biological systems, the interesting oxidative chemistry of Cu including the relatively rare Cu(III) valence state illustrates how in both model and enzyme systems the X-ray absorption edge provides direct electronic structural information. Building on an earlier study that defined a means of identification and quantification of Cu(I) and Cu(II) in biological systems (Kau *et al.*, 1987), a recent study of a number of Cu(III) complexes as well as species produced by ligand-based oxidation shows that this higher-valent oxidation state can be probed as well (DuBois *et al.*, 1997; Yang *et al.*, 1998). The results demonstrate that the Cu *K*-edge is a reliable indicator for Cu(III); the edges for Cu(III) species show a systematic shift to higher energy, with the energy position of the 1*s*–3*d* transition being very diagnostic of Cu(III) *versus* Cu(II). A more detailed analysis of 1*s*–4*p* transitions in specific pairs of Cu(II)/Cu(III) edges reveals the strongly covalent nature of the Cu(III) oxide bond. XAS edge studies can therefore be used as a means of distinguishing Cu(II), Cu(III) and Cu(II)-oxidized ligand systems.

In an example of a specific biological application, Fig. 4 shows the X-ray absorption *K*-edge spectra of oxidized and reduced forms of superoxide dismutase for the Cu and Zn sites of the enzyme. The changes in the Zn *K*-edge spectra

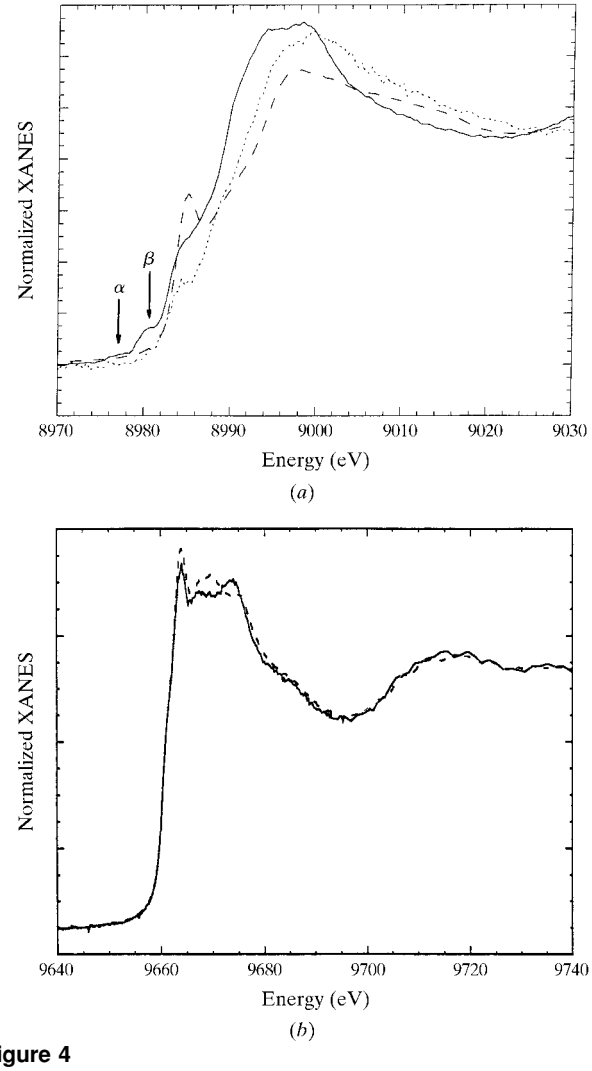


**Figure 4**
XANES of Cu-Zn bovine superoxide dismutase at the (*a*) Cu and (*b*) Zn *K*-edges. The data are for oxidized (solid line) and reduced (dashed line) enzyme in solution. For the Cu *K*-edge, data for a slurry of crystals are also shown (dotted line); in this case the mixed oxidation state of the Cu sites is clearly evident and can be simulated by simple averaging of the oxidized and reduced spectra.

upon reduction of the enzyme are subtle, confirming that very small changes take place in the bridging His ligand's geometry at the Zn site. In contrast, the Cu data show a major change. The features, marked $\alpha$ and $\beta$, are absent in the reduced Cu site and are consistent with the $Cu^{+}$ redox state. Furthermore, the appearance of a distinct peak at 8984 eV in the reduced enzyme is a characteristic feature observed for a three-coordinate Cu(I) site with trigonal geometry (Kau *et al.*, 1987; Blackburn *et al.*, 1989), thus confirming that, upon reduction, the bridging imidazole His 61 is protonated and that Cu moves to form a trigonal geometry with the remaining three His ligands. In a recent high-resolution (1.65 Å) crystallographic study of bovine superoxide dismutase, Cu-Zn sites of one of the monomers in this homo-dimer enzyme were found to be those expected for the reduced enzyme even though no attempt was made to reduce the protein or the crystals (Hough & Hasnain, 1999; see also §4.3.2). This one-site-reduced and one-site-oxidized state of the enzyme was confirmed by obtaining XANES data on a slurry of these crystals and is shown in Fig. 4. This specific example illustrates that use of XANES is important in defining the oxidation state of the metal centre in a crystallographic study as well as for relating it to the solution state. The use of XANES may also prove useful in separating kinetically different states of the enzyme in a 'time-resolved' crystallographic study.

4.1.2. *L-edge XANES and $K_\beta$-fluorescence*. There are several newer developments that hold promise for providing additional electronic structural information on metal centres utilizing absorption-edge information. Recent studies have shown that $K_\beta$ emission lines are exquisitely sensitive to oxidation states. With appropriate instrumentation to provide very high energy resolution, it is possible to obtain information from XAS spectra even when more than one oxidation state of an element is present (Wang *et al.*, 1997). Such studies are especially useful for transition metal complexes in mixed-valent and redox active centres (Bergmann *et al.*, 1998). *L*-edges are also useful in interrogation of electronic structure of the transition metals as they have intrinsically good resolution compared with the comparable *K*-edge of the same element (due to reduced core-hole lifetime and monochromator resolution effects) and directly probe the *d*-manifold through the allowed *p–d* transitions. Such studies may be applied in the normal 'absorption mode' or circularly polarized radiation can be utilized in an 'XMCD' experiment where one can obtain sensitivity to orbital and spin angular momentum (Wang *et al.*, 1998).

### 4.2. *Early experiments and their impact on MAD*

The so-called anomalous scattering terms in X-ray diffraction are directly related to the X-ray absorption process. Specifically, the imaginary part $f''$ is directly proportional to $\omega$ times the total absorption cross section, and $f'$, the real component, is related to it by the Kramer–Krönig dispersion relationship. Many years ago it was recognized that anomalous scattering could be used to solve the classic phase problem in protein crystallography (Bijvoet *et al.*, 1951), but in practice the relatively small magnitude of anomalous-scattering terms and the lack of tunability of conventional sources limited significantly their practical application until the availability of synchrotron radiation in the mid-to-late 1970s. The readily tunable nature of synchrotron radiation generated a renaissance of interest in the study and use of anomalous scattering. It was shown that near absorption threshold, changes in $f'$ and $f''$ did not exhibit behaviour predicted by atomic theory (see *e.g.* Phillips *et al.*, 1978). Rather, there were large resonance and molecular effects that gave rise to often dramatic and large changes in their values. X-ray absorption edges were measured for a number of metal complexes and from these measurements anomalous-scattering terms were derived. For example, the lanthanides were found to give changes in anomalous terms by as much as 20 electrons with only a few eV change in energy (Lye *et al.*, 1980). An example of the dramatic nature of these changes is illustrated in Fig. 5 where the values of $f'$ and $f''$ around the $L_2$ and $L_3$ edges of an Eu complex are shown. It became very clear that such large effects provided powerful phasing power that could be used to solve the crystallography phase problem for many structures. For a discussion of this approach, its development and relevant references, see Phillips & Hodgson (1980) and Doniach *et al.* (1997). Indeed, the multiwavelength anomalous scattering phasing (the MAD technique) has become one of the mainstream approaches

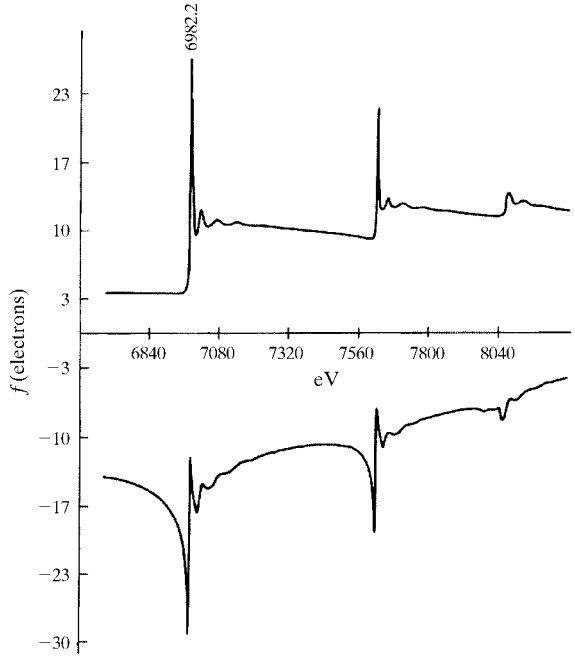


**Figure 5**
Measurements around the *L* edges of a Eu complex show the very large changes in values of $f'$ and $f''$, for $L_2$ and $L_3$ edges, that can be used to provide significant phasing power when used in the multiple-wavelength anomalous dispersion (MAD) approach to phase determination. The upper panel provides $f''$ and lower $f'$.

currently used in protein crystallography (Hendrickson, 1991; and articles in this issue).

### 4.3. *Some recent EXAFS applications*

Before we discuss any specific examples, we need to ask ourselves why use XAFS when protein crystallography has become a 'routine' technique. The major strengths of EXAFS, namely that of atomic or even subatomic resolution and its equal applicability to solution and solid-state samples, have already been mentioned. In this section, several examples are used to illustrate how these advantages manifest themselves in real systems and, as such, each represents a different case. Here, we have concentrated on copper and molybdenum proteins due to our own scientific interest. Each of the examples is chosen to illustrate the synergy between the two techniques. The examples are all recent and some are even as yet unpublished and, as such, represent the current state of affairs of the techniques.

Tables 3 and 4 provide details of the highest resolution structures, which are currently available for copper- and molybdenum-containing proteins. There are a total of 165 structures known for copper proteins but only amicyanin (MW ~11.5 kDa) and plastocyanin (10.5 kDa), both cupredoxins, have been determined to a resolution approaching atomic resolution, namely 1.3 and 1.33 Å, respectively. For molybdenum proteins, the highest resolution structure is that of DMSO reductase (~85 kDa) which is known to only 1.82 Å, well away from the 'atomic' resolution.

4.3.1. *Cupredoxins*. A family of functionally related metalloproteins, known as 'blue' copper proteins (or Cupredoxins), mediate electron transfer, a fundamental biological process. These proteins have attracted much attention as model electron-transfer proteins because of their relative simplicity, their richness in electronic spectra (colour, in fact the colour could be blue to green) and their accessibility by a variety of physical methods (Adman & Jensen, 1981; Reinhammar, 1979). The crystallographic structure of several of these have been determined at a variety of resolutions (Adman & Jensen, 1981; Nar *et al.*, 1991; Guss & Freeman, 1983; Guss *et al.*, 1992; Baker, 1988; Norris *et al.*, 1983; Dodd *et al.*, 1995). The coordination sphere around copper consists of two N atoms (residues His-117 and His-46 in the case of azurins) and two sulfur donors (residues Cys-112 and Met-121).

Fig. 6 shows a comparison of EXAFS data for the oxidized and reduced forms of azurin. There is a clear change in frequency of the two spectra providing direct evidence for a change in Cu–ligand distances upon reduction. A detailed analysis shows that the extent of the change is very significant from the EXAFS point of view and is what will be expected from the removal/addition of a single electron. An increase in the $Cu-S_{cys}$ bond and in the $Cu-N_{His}$ distances is observed in the EXAFS of reduced protein. These changes are compared with the crystallographic values for the oxidized and reduced form of azurin (Dodd & Hasnain, unpublished results), Table 5. This comparison reveals a general agreement between the two techniques, with the agreement for the $Cu-S_{cys}$ distance being excellent. We, however, note that the Cu—His distance for the native oxidized protein is systematically longer in the crystal structure by about 0.1 Å. A similar discrepancy is found in other cupredoxins where better agreement for the $Cu-S_{cys}$ bond distance is found between the two techniques. The reason for this discrepancy is unknown and further work is required. A high-resolution crystallographic study as well as a single-crystal XAFS study of the same crystal would be particularly helpful in this respect. The very small changes observed upon reduction for these ligands in the crystallographic studies is well within the accuracy of the structure

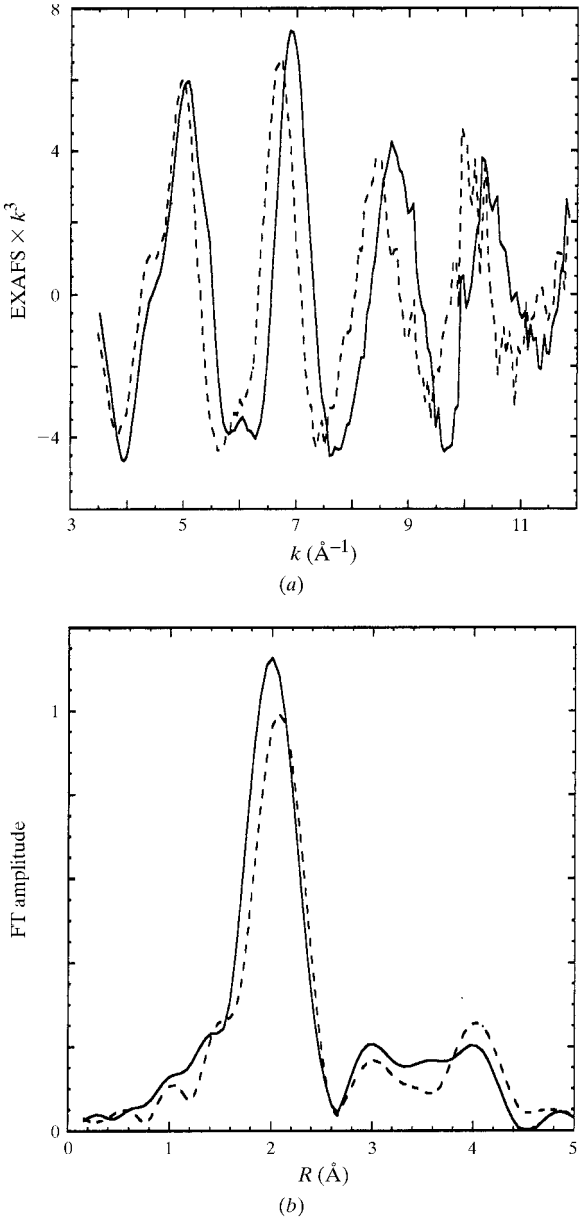


**Figure 6**
EXAFS (*a*) and Fourier transforms (*b*) of azurin II from *Alcaligenes xylosoxidans* in oxidized (solid line) and reduced (dashed line) forms.

(Cruickshank, 1999) and cannot be justified in the absence of independent metrical information from EXAFS. This is an example where a combination of high-resolution crystallographic studies (~1.75 Å) and EXAFS is able to define the structural changes resulting from reduction, *i.e.* movement of a single electron.

4.3.2. *Cu-Zn superoxide dismutase*. Superoxide dismutases are a ubiquitous family of functionally related enzymes responsible for the removal of toxic radical superoxide in biological systems. The widely accepted mechanism of superoxide dismutation [equations (1) and (2)] involves a cyclic reduction of Cu(II) and oxidation of Cu(I),

$$O_2^- + \text{Enz-Cu}^{2+} \rightarrow O_2 + \text{Enz-Cu}^{+} \qquad (1)$$

$$\text{Enz-Cu}^{+} + O_2^- + 2H^+ \rightarrow \text{Enz-Cu}^{2+} + H_2O_2. \qquad (2)$$

A 2 Å resolution crystal structure of the oxidized bovine Cu-Zn SOD was published in 1982 (Tainer *et al.*, 1982) which showed that the active site consisted of a binuclear site where the Cu(II) and Zn(II) ions were bridged by an imidazolate ring, His-61. The copper ion was found to be coordinated to four histidine residues arranged in a distorted square pyramid with a water molecule located at ~3 Å. The zinc ion was found to be coordinated by three histidine residues and an aspartate in a distorted tetrahedron. Based on this structure, Tainer *et al.* proposed a detailed mechanism of dismutation in 1983 (Tainer *et al.*, 1983), which involved the dissociation of the Cu-His61 bond upon reduction. The presence of three-coordinate copper in the reduced form had been suspected from many spectroscopic studies and its first structural evidence was provided by EXAFS in 1984 (Blackburn *et al.*, 1984). It took another ten years before the first crystallographic structure of reduced SOD became available; but surprisingly this showed the coordination of both Cu and Zn to remain unchanged (Rypniewski *et al.*, 1995). XANES data clearly shows that the Cu site adopts a trigonal geometry upon reduction. This lowering of coordination is also clearly evident in the EXAFS region as has been shown by Blackburn *et al.* (1984) and Murphy *et al.* (1997).

Recently, Hough & Hasnain (1999) have determined the structure of bovine Cu-ZnSOD in two crystal forms, $P2_12_12_1$ (1.65 Å resolution) and $C222_1$ (2.3 Å resolution). In the 2.3 Å structure, both monomers are in the oxidized state while, in the 1.65 Å structure, monomer A is in the reduced state and the Cu is tricoordinate, having lost the coordinated water molecule and His 61 from ligation (Hough & Hasnain, 1999). In the reduced site, a clear movement of Cu in the plane of coordinating N atoms is observed together with a rotation of His 61 away from Cu. Cu—N(His 61) in the reduced site is 3.1 Å, Fig. 7. Interestingly, the Cu—Zn distance in the reduced form is increased by ~0.6–0.7 Å. The mixed state (one site reduced and one oxidized) is confirmed by the XANES data obtained from a crystalline slurry, Fig. 4. The evidence for a tricoordinate Cu site has also been provided in yeast SOD (Ogihara *et al.*, 1996).

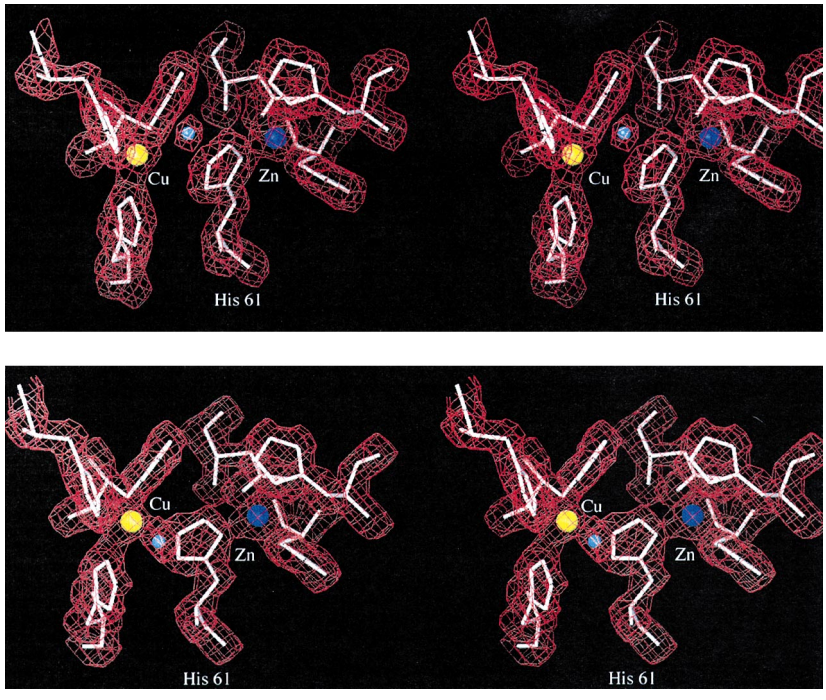


**Figure 7**
A stereoview of the Cu and Zn sites in two monomers of bovine Cu-Zn SOD 1.65 Å resolution structure. Monomer *a* (top) is clearly tricoordinate showing a clear break between Cu and His 61 while monomer *b* (bottom) shows this bond intact and a well defined water density at the Cu site. Cu and Zn molecules are shown as yellow and blue spheres, respectively. A water molecule is shown as a smaller blue sphere.

**Table 3**
Highest resolution X-ray structures of copper proteins.

There are a total 165 copper protein structures in the PDB (1 April 1999).

| PDB ref. | Protein | Author | MW (kDa) | Resolution (Å) |
|---|---|---|---|---|
| Single copper proteins | | | | |
| 1AAC | Amicyanin (ox) | Cunane & Chen (1996) | 11.5 | 1.31 |
| 1BXA | Amicyanin (red pH 4.4) | Zhu *et al.* (1999) | 11.5 | 1.30 |
| 1PLC | Plastocyanin (ox pH 6.0) | Guss *et al.* (1992) | 10.5 | 1.33 |
| 1PMY | Pseudoazurin | Inoue & Kai (1994) | 13.4 | 1.50 |
| 1JER | Cucumber stellacyanin | Hart & Nersissian (1996) | 20.0 | 1.60 |
| Multi-copper proteins | | | | |
| 1NIF | Cu-nitrite reductase | Adman & Godden (1995) | 110 | 1.60 |
| 1GOF | Galactose oxidase (pH 4.5) | Ito *et al.* (1991) | 68 | 1.70 |
| Cu-Zn proteins | | | | |
| 1JCV | Reduced yeast CuZn SOD | Ogihara *et al.* (1996) | 32 | 1.55 |
| 1CBJ | Bovine superoxide dismutase | Hough & Hasnain (1999) | 32 | 1.65 |

This is an example which illustrates the importance of ensuring the integrity of a reaction state (native or an intermediate stable functional state) in the crystal. It is important to remember that it is not sufficient to carry out control on a crystal of the same batch. This does, indeed, argue for the need of an on-line monitoring. For metalloproteins, the on-line recording of XANES data can ideally provides this, as these data can be obtained for any metal in any oxidation state. Optical or EPR data are useful supplementary information but are limited to only the electronically active state; thus Cu(I) or Zn, for example, have no optical or EPR signals.

This example shows a different aspect of the synergy between the two techniques. Even though XAFS has provided a consistent picture of the reduced state of the enzyme, the detailed movements, namely the movement of Cu, rotation of His 61 away from Cu and increased separation of Cu and Zn, have only been defined by crystallography (Hough & Hasnain, 1999).

4.3.3. *Mo oxo enzymes*. There is a large class of oxotransferase and hydroxylase enzymes containing molybdenum (Hille, 1996) or tungsten (Johnson *et al.*, 1996) which catalyse the generalized reaction

$$X + H_2O \rightarrow XO + 2H^+ + 2e^-$$

involving substrate and product *X*/*X*O. For all of these enzymes where structures are known, the mononuclear molybdenum or tungsten ion is coordinated by one or two pterin co-factors. The molybdoenzymes are usually classified into three families (xanthine oxidase, sulfite oxidase and DMSO reductase) depending upon the number of co-factor ligands on the metal and if the $Mo^{VI}OS$ group is present in the oxidized form of the enzyme. Studies by spectroscopy (most notably EPR and EXAFS) and protein crystallography have been used to investigate the structure and function of a variety of members of this enzyme family. The interpretation of X-ray crystallography results on metalloproteins containing single heavy metals like Mo (or W) can have problems, especially at lower resolutions, as discussed by Rees and co-workers (Schindelin *et al.*, 1997). As noted earlier, EXAFS can provide an accurate metrical probe of local structure and such studies are complementary to the crystallography; hence, the value of applying both methods to a given problem becomes apparent. This approach is well illustrated by the studies on DMSO reductase.

In the DMSO reductase family of enzymes a number of X-ray crystal structures and EXAFS studies have been made. X-ray crystal structures of the oxidized and reduced forms of the DMSO reductases from *Rhodobacter sphaeroides* (Schindelin *et al.*, 1996) and *Rhodobacter capsulatus* (Schneider *et al.*, 1996; McAlpine *et al.*, 1997) have been determined. McAlpine *et al.* (1998) has also published the structure of a DMSO-bound complex. EXAFS studies have been made of these DMSO reductases as well (George *et al.*, 1999; Baugh *et al.*, 1997). It is interesting that, among the three crystal structures, all contain two pterin dithiolene co-factors and a serine side chain ligated to the Mo. However, they show differing numbers of Mo═O groups and significant differences in the coordination of the pterin ligands. Crystallographic (McAlpine *et al.*, 1997) and EXAFS (Baugh *et al.*, 1997) studies on DMSO reductase from *Rhodobacter capsulatus* were the first to demonstrate that all four S atoms from the two pterin ligands were bound to Mo. George *et al.* (1999) in an independent EXAFS study has confirmed this. Despite a significant agreement between the two EXAFS studies, these give somewhat differing results regarding the number of oxygen ligands, agreeing qualitatively with one or the other of the structures determined crystallographically. George *et al.* (1999) have shown that a monooxo Mo site is present that converts to a Mo—O ligand when reduced. While there is some difference in the details, the analysis of Garner and co-workers (Baugh *et al.*, 1997) also appears to be consistent with this picture. Thus the EXAFS studies are not consistent with a dioxo oxidized or a monooxo reduced active site as suggested in one of the crystallographic studies (McAlpine *et al.*, 1997). Indeed, among the crystal

**Table 4**
Highest resolution X-ray structures of molybdenum proteins.

There are currently a total of 16 structures of molybdenum proteins in the PDB (1 April 1999).

| PDB ref | Protein | Author | MW (kDA) | Resolution (Å) |
|---|---|---|---|---|
| 1DMR | DMSO reductase (ox) | McAlpine *et al.* (1997) | 85 | 1.82 |
| 1DMS | DMSO reductase | Schneider *et al.* (1996) | 85 | 1.88 |
| 1ALO | Aldehyde oxidoreductase | Romao *et al.* (1995) | 132 | 2.00 |
| 2MIN | Nitrogenase MoFe | Peters *et al.* (1997) | 240 | 2.03 |
| 1AA6 | Formate dehydrogenase | Boyington *et al.* (1997) | 79 | 2.30 |

**Table 5**
A comparison of EXAFS and crystallographic structural parameters for the oxidized and reduced azurin II from *Alcaligenese xylosoxidans*.

The EXAFS values for $S_\delta$ are uncertain and arrived at when included in the model at the crystallographic positions before refinement. Accuracy of metrical information from EXAFS for Cu—S$\gamma$ is about ±0.01 Å, for His $N_\delta$ is about ±0.02 Å. The DPIs [diffraction-component precision indicator as defined by Cruickshank (1999)] for the refinement of oxidized and reduced AzII at 1.75 Å are 0.09 and 0.08 Å, respectively.

| | Crystallographic (1.75 Å)† | | EXAFS‡ | |
|---|---|---|---|---|
| Cu ligand | Oxidized | Reduced | Oxidized | Reduced |
| 46 $N_\delta$ | 2.04 | 2.03 | 1.93 | 1.90 |
| 117 $N_\delta$ | 1.99 | 2.02 | 1.93 | 2.01 |
| 112 S$\gamma$ | 2.14 | 2.16 | 2.10 | 2.17 |
| 45 O | 2.74 | 2.84 | 2.71 | 2.90 |
| 121 $S_\delta$ | 3.28 | 3.28 | 3.40 | 3.55 |

† Dodd & Hasnain (unpublished results). ‡ Strange, Cheung & Hasnain (unpublished results).

structures there are discrepancies on structural issues including significant structural differences between enzymes with the same function, and unusual metal–ligand binding features such as asymmetric pterin co-factor coordination and associated highly irregular coordination units. It is possible that these structures represent different oxidation states. It is clear that this is a complex story without complete resolution at this time, but it does illustrate clearly the need to use all available tools, if at all possible, on the same samples in order to understand the structure and function of metalloprotein active sites where accurate metrical and electronic structural information are essential and not often available from X-ray crystallography alone.

## 5. Conclusions

EXAFS and XANES can provide very high resolution (<0.2 Å) structural information in both crystalline and aqueous states for the metal centres in a protein. The resolution at which this information is achieved is the same in the two states and in fact is the same as that routinely achieved in 'small molecule' crystallography. The agreement between XAFS and crystallography is excellent for small molecules and is usually ±0.01 Å for ligating atoms. However, this agreement is rather limited in the case of proteins mainly because of the lower resolution of the protein structures (generally >1.5 Å). The resolution of the protein X-ray structures can be expected to improve with the improvement in synchrotron radiation sources and detectors but, for a foreseeable future, XAFS will continue to be an important structural tool for structure–function studies of metalloproteins. Even at atomic resolutions, *i.e.* at <1.2 Å, structural changes associated with movement of an electron (redox processes) may not be defined with complete confidence. It is at these subatomic resolutions that XAFS is likely to maintain its uniqueness in studying structure–function relationships in metalloproteins in both solution and crystalline states. Furthermore, XAFS interrogates directly metal atom oxidation state and electronic structure, information that can only be inferred from crystallography. Hence, it has an additional important role to play, namely that of acting as a control in order to ensure the integrity of the given oxidation state of a protein crystal. If the dream of a 'structural movie' is to be realised, then on-line monitoring by XAFS should be an integral part of such crystallographic experiments on metalloproteins. It is only through the rigour of these experiments that we would be able to provide structural data of quality to underpin the chemistry/biochemistry of this class of proteins.

We would like to thank our colleagues, collaborators and the current and past members of our groups.

## References

Adman, E. T., Godden, J. W. & Turley, S. (1995). *J. Biol. Chem.* **270**, 27458–27474.
Adman, E. T. & Jensen, L. H. (1981). *Isr. J. Chem.* **21**, 8–12.
Ascone, I., Castamer, R., Bolognesi, M., Tarricone, C., Strappolo, M. E. & Desideri, A. (1997). *Biochem. Biophys. Res. Commun.* **241**(1), 119–121.
Ashley, C. A. & Doniach, S. (1975). *Phys. Rev. B*, **11**, 1279–1288.
Baker, E. N. (1988). *J. Mol. Biol.* **203**, 1071–1075.
Bau, R., Rees, D. C., Kurtz, D. M., Scott, R. A., Huang, S., Adams, M. W. W. & Eidsness, M. (1998). *J. Biol. Inorg. Chem.* **3**, 484–495.
Baugh, P. E., Garner, C. D., Charnock, J. M., Collison, D., Davies, E. S., McAlpine, A. S., Bailey, S., Lane, I., Hanson, G. R. & McEwan, A. G. (1997). *J. Biol. Inorg. Chem.* **2**, 634–643.

Bergmann, U., Grush, M. M., Horne, C. R., DeMarois, P., Penner-Hahn, J. E., Yocum, C. F., Wright, D. W., Dubé, C. E., Armstrong, W. H., Christou, G., Eppley, H. J. & Cramer, S. P. (1998). *J. Phys. Chem.* B**102,** 8350.
Bianconi, A., Congiu-Castellano, A., Durham, P. J., Hasnain, S. S. & Phillips, S. (1985). *Nature (London)*, **318**, 685–687.
Bijvoet, J. M., Peerdeman, A. F. & von Brommel, A. J. (1951). *Nature (London)*, **168**, 271–272.
Binsted, N. & Hasnain, S. S. (1996). *J. Synchrotron Rad.* **3**, 185–196.
Binsted, N., Strange, R. W. & Hasnain, S. S. (1992). *Biochemistry*, **31**, 12117–12125.
Blackburn, N. J., Hasnain, S. S., Binsted, N., Diakun, G. P., Garner, C. D. & Knowles, P. F. (1984). *Biochem. J.* **219**, 985–990.
Blackburn, N. J., Strange, R. W., McFadden, L. M. & Hasnain, S. S. (1987). *J. Am. Chem. Soc.* **109**, 7162–7170.
Blackburn, N. J., Strange, R. W., Reedijk, J., Volbeda, A., Farooq, A., Karlin, K. D. & Zubieta, J. (1989). *Inorg. Chem.* **28**, 1349.
Bordas, J., Bray, R. C., Garner, C. D., Gutteridge, S. & Hasnain, S. S. (1979). *J. Inorg. Biochem.* **11**, 181–184.
Bordas, J., Bray, R. C., Garner, C. D., Gutteridge, S. & Hasnain, S. S. (1980). *Biochem. J.* **191**, 499–508.
Boyington, J. C., Gladyshev, V. N., Kjangulov, S. V., Stadtman, T. C. & Sun, P. D. (1997). *Science*, **275**, 1305–1308.
Brodersen, D. E., Etzerodt, M., Madsen, P., Celis, J. E., Thogersen, H. C., Nyborg, J. & Kjeldgaard, M. (1998). *Structure*, **6**, 477–489.
Cassetta, A., Deacon, A., Ealick, S., Helliwell, J. R. & Thompson, A. W. (1999). *J. Synchrotron Rad.* **6**, 822–833.
Chu, K., Berendzen, J., Schlichting, I., Sweet, R. M. & Vojtechovsky, J. (1998). *Biophys. J.* **74**, 236.
Co, M. S., Hendrickson, W. A., Hodgson, K. O. & Doniach, S. (1983). *J. Am. Chem. Soc.* **105**, 1144–1150.
Cramer, S. P., Dawson, J. H., Hodgson, K. O. & Hager, L. P. (1978). *J. Am. Chem. Soc.* **100**, 7282–7290.
Cramer, S. P. & Hodgson, K. O. (1979). *Prog. Inorg. Chem.* **25**, 1–39.
Cramer, S. P., Hodgson, K. O., Gillum, W. O. & Mortensen, L. E. (1978). *J. Am. Chem. Soc.* **100**, 3398–3407.
Cramer, S. P., Tench, O., Yocum, M. & George, G. N. (1988). *Nucl. Instrum. Methods*, A**266**, 586–591.
Cruickshank, D. W. J. (1999). *Acta Cryst.* D**55**, 583–601.
Cunane, L. M., Chen, Z. W., Durley, R. C. E. & Mathews, F. S. (1996). *Acta Cryst.* D**52**, 676–686.
Dauter, Z., Butterworth, S., Sieker, L. C., Sheldrick, G. & Wilson, K. S. (1997). Unpublished.
Dauter, Z., Lamzin, V. S. & Wilson, K. O. (1997). *Curr. Opin. Struct. Biol.* **7**, 681–688.
Dauter, Z., Wilson, K. S., Sieker, L. C., Meyer, J. & Moulis, J. M. (1997). *Biochemistry*, **36**, 16065–16073.
Dauter, Z., Wilson, K. S., Sieker, L. C., Moulis, J. M. & Meyer, J. (1996). *Proc. Natl Acad. Sci. USA*, **93**, 8836–8840.
Deacon, A. M., Gleichmann, T., Kalb, A. J., Price, H., Raferty, J., Bradbrook, G., Yariv, J. & Helliwell, J. R. (1997). *J. Chem. Soc. Faraday Trans.* **93**, 4305–4312.
Declerq, J. P., Evrard, J., Carter, D. C., Wright, B. S., Etienne, G. & Parello, J. (1999). *J. Crystal Growth*, **196**, 595–691.
Derbyshire, G. E., Cheung, K. C., Sangsingkeow, P. & Hasnain, S. S. (1999). *J. Synchrotron Rad.* **6**, 62–63.
Derbyshire, G. E., Dent, A. J., Dobson, B. R., Farrow, R. C., Felton, A., Greaves, G. N., Morrell, C. & Wells, M. P. (1992). *Rev. Sci. Instrum.* **63**, 814–815.
Dodd, F. E., Hasnain, S. S., Abraham, Z. H. L., Eady, R. R. & Smith, B. E. (1995). *Acta Cryst.* D**51**, 1052–1064.
Doniach, S., Hodgson, K., Lindau, I., Pianetta, P. & Winick, H. (1997). *J. Synchrotron Rad.* **4**, 380–395.
DuBois, J. L., Mukherjee, P., Collier, A. M., Mayer, J. M., Solomon, E. I., Hedman, B., Stack, T. D. P. & Hodgson, K. O. (1997). *J. Am. Chem. Soc.* **119**, 8578–8579.
Durham, P. J., Pendry, J. B. & Hodges, C. H. (1981). *Solid State Commun.* **38**, 159–162.
Filipponi, A., DiCicco, A. & Natoli, C. R. (1995). *Phys. Rev. B*, **52**, 15122–15134.
Foulis, D. L., Pettifer, R. F., Natoli, C. R. & Benfatto, M. (1990). *Phys. Rev.* A**41**, 6922–6927.
Frahm, R. (1989). *Rev. Sci. Instrum.* **60**, 2515–2518.
Frazao, C., Soares, C. M., Carrondo, M. A., Pohl, E., Dauter, Z., Wilson, K. S., Hervas, M., Navarro, J. A., Delarosa, M. A. & Sheldrick, G. M. (1995). *Structure*, **3**, 1159–1169.
Garner, C. D. & Hasnain, S. S. (1981). *Proceedings of the First EXAFS Conference*, DL/Sci/R17. Warrington: Daresbury Laboratory.
George, G. N., Hilton, J., Temple, C., Prince, R. C. & Rajagopalan, K. V. (1999). *J. Am. Chem. Soc.* **121**, 1256–1266.
Goulon, J., Goulon-Ginet, C. & Brookes, N. (1997). *J. Phys.* **7**, Vols. 1 and 2.
Gurman, S. J., Binsted, N. & Ross, I. (1984). *J. Phys. C.* **17**, 143–151.
Gurman, S. J., Binsted, N. & Ross, I. (1986). *J. Phys. C.* **19**, 1845–1861.
Guss, J. M., Bartunik, H. D. & Freeman, H. C. (1992). *Acta Cryst.* B**48**, 790–811.
Guss, J. M. & Freeman, H. C. (1983). *J. Mol. Biol.* **169**, 521–563.
Harata, K., Abe, Y. & Muraki, M. (1999). *J. Mol. Biol.* **287**, 347–358.
Harrison, P. M. (1985). *Metalloproteins*, Parts I and II. New York: Academic Press.
Hart, P. J., Nersissian, A. M., Herrmann, R. G., Nalbandyan, R. M., Valentine, J. S. & Eisenberg, D. (1996). *Protein Sci.* **5**, 2175–2183.
Hasnain, S. S. & Strange, R. W. (1990). In *Synchrotron Radiation and Biophysics.* Chichester: Ellis Horwood.
Hendrickson, W. (1991). *Science*, **254**, 51–58.
Hille, R. (1996). *Chem. Rev.* **96**, 2757–2816.
Hough, M. A. & Hasnain, S. S. (1999). *J. Mol. Biol.* **287**, 579–592.
Hu, Z., Kaindl, G., Warda, S. A., Reinen, D., de Groot, F. M. F. & Muller, B. G. (1998). *Chem. Phys.* **232**, 63–74.
Inoue, T., Kai, Y., Harada, S., Kasai, N., Ohshiro, Y., Suzuki, S., Kohzuma, T. & Tobari, J. (1994). *Acta Cryst.* D**50**, 317–328.
Ito, N., Phillips, S. E. V., Stevens, C>, Ogel, Z. B., McPherson, M. J., Keen, J. N., Yadav, K. D. S. & Knowles, P. F. (1991). *Nature (London)*, **350**, 87–90.
Jaklevic, J., Kirby, J. A., Klein, M. P., Robertson, A. S., Brown, G. S. & Eisenberger, P. (1977). *Solid State Commun.* **23**, 679–682.
Johnson, M. K., Rees, D. C. & Adams, M. W. W. (1996). *Chem. Rev.* **96**, 2817–2839.
Joly, Y. (1997). *J. Phys.* **7**(C2), 111–115.
Kachalova, G. S., Popov, A. N., & Bartunik, H. D. (1999). *Science*, **284**, 473–476.
Kau, L., Spira-Solomon, D., Penner-Hahn, J. E., Hodgson, K. O. & Solomon, E. I. (1987). *J. Am. Chem. Soc.* **109**, 6433–6442.
Kendrew, J. C., Bodo, G., Dintzis, H., Parrish, R. G., Wyckoff, H. & Phillips, D. C. (1958). *Nature (London)*, **181**, 662.
Kincaid, B. & Eisenberger, P. (1975). *Phys. Rev. Lett.* **34**, 1361–1364.
Lee, P. A. & Pendry, J. B. (1975). *Phys. Rev. B*, **11**, 2795–2811.
Liu, H. I., Filipponi, A., Gavini, N., Burgess, B. K., Hedman, B., DiCicco, A., Natoli, C. R. & Hodgson, K. O. (1994). *J. Am. Chem. Soc.* **116**, 2418–2423.
Louie, G. V. & Brayer, G. D. (1990). *J. Mol. Biol.* **214**, 527–555.
Lye, R. C., Phillips, J. C., Kaplan, D., Doniah, S. & Hodgson, K. O. (1980). *Proc. Natl Acad. Sci. USA*, **77**, 5884–5888.
Lytle, F. (1999). *J. Synchrotron Rad.* **6**, 123–134.
McAlpine, A. S., McEwan, A. G. & Bailey, S. (1998). *J. Mol. Biol.* **275**, 613–623.
McAlpine, A. S., McEwan, A. G., Shaw, A. & Bailey, S. (1997). *J. Biol. Inorg. Chem.* **2**, 690–701.

Murphy, L. M., Dobson, B. R., Neu, M., Ramsdale, C. A., Strange, R. W. & Hasnain, S. S. (1995). *J. Synchrotron Rad.* **2**, 64–69.
Murphy, L. M., Strange, R. W. & Hasnain, S. S. (1997). *Structure*, **5**, 371–379.
Murphy, L. M., Strange, R. W., Karlson, G., Lundberg, L., Reinhammar, B. & Hasnain, S. S. (1993). *Biochemistry*, **32**, 1965–1975.
Mustre de Leon, J., Yacoby, Y., Stern, E. A. & Rehr, J. J. (1990). *Phys. Rev. B*, **42**, 10843–10851.
Nar, H., Messerschmidt, A., Huber, R., van de Kamp, M. & Canters, G. W. (1991). *J. Mol. Biol.* **221**, 765–772.
Norris, G. E., Anderson, B. F. & Baker, E. N. (1983). *J. Mol. Biol.* **165**, 501.
Ogihara, N., Parge, H. E., Hart, P. J., Weiss, M. S., Goto, J. J., Crane, B. R., Tsang, J., Slater, K., Roe, J. A., Valentine, J. S., Eisenberg, D. & Tanier, J. A. (1996). *Biochemistry*, **35**, 2316–2321.
Parkin, S., Tupp, B. & Hope, H. (1996). *Acta Cryst.* D**52**, 1161–1168.
Pendry, J. B. (1974). *Low Energy Electron Diffraction.* New York: Academic Press.
Perutz, M. F. (1970). *Nature (London)*, **228**, 726.
Perutz, M. F., Hasnain, S. S., Duke, P. J., Sessler, J. L. & Hahn, J. E. (1982). *Nature (London)*, **295**, 535–538.
Peters, J. W., Stowell, M. H. B., Soltis, S. M., Finnegan, M. G., Johnson, M. K., Popov, A. N., Kachalova, G. S. & Bartunik, H. H. (1997). *Biochemistry*, **36**, 1181–1187.
Pettifer, R. F., Foulis, D. L. & Hermes, C. (1986). *J. Phys. C*, **8**, 545–548.
Phillips, J. C. & Hodgson, K. O. (1980). *Acta Cryst.* A**36**, 856–864.
Phillips, J. C., Templeton, D. H., Templeton, L. K. & Hodgson, K. O. (1978). *Science*, **201**, 257–259.
Rehr, J. J., Booth, C. H., Bridges, F. & Zabinsky, S. I. (1994). *Phys. Rev. B*, **49**, 12347–12350.
Reinhammar, B. (1979). *Advances in Inorganic Biochemistry*, edited by G. L. Eichhorn & L. G. Marzelli, p. 92. North Holland: Elsevier.
Romao, M. J., Archer, M., Moura, I., Moura, J. J. G., Legall, J., Engh, R., Schneider, M., Hof, P. & Huber, R. (1995). *Science*, **270** 1170–1176.
Rosenbaum, G., Holmes, K. C. & Wiltz, J. (1971). *Nature (London)*, **230**, 434–437.
Rypniewski, W. R., Mangani, S., Bruni, B., Orioli, P. L., Casati, M. & Wilson, K. S. (1995). *J. Mol. Biol.* **251**, 282–296.
Sayers, D. E., Stern, E. & Lytle, F. (1971). *Phys. Rev. Lett.* **27**, 1204–1207.
Schindelin, H., Kisker, C., Hilton, J., Rajagopalan, K. V. & Rees, D. C. (1996). *Science*, **272**, 1615–1621.
Schindelin, H., Kisker, C. & Rees, D. C. (1997). *J. Biol. Inorg. Chem.* **2**, 773–781.
Schneider, F., Löwe, J., Huber, R., Schindelin, H., Kisker, C. & Knäblein, J. (1996). *J. Mol. Biol.* **263**, 53–69.
Scott, R. A., Hahn, J. E., Doniach, S., Freeman, H. C. & Hodgson, K. O. (1982). *J. Am. Chem. Soc.* **104**, 5364–5369.
Schulman, R. G., Eisenberger, P., Blumberg, W. E. & Stombaugh, N. A. (1975). *Proc. Natl Acad. Sci. USA*, **72**, 4003–4007.
Shiro, Y., Obayashi, E., Adachi, S. I., Iizuka, T., Nomura, M. & Shoun, H. (1997). *J. Phys.* **7**, 587–591.
Stern, E. A. (1974). *Phys. Rev. B*, **10**, 3027–3037.
Stout, C. D., Stura, E. A. & McRee, D. E. (1998). *J. Mol. Biol.* **278** 629–639.
Strange, R. W., Blackburn, N. J., Knowles, P. F. & Hasnain, S. S. (1987). *J. Am. Chem. Soc.* **109**, 7157–7162.
Tainer, J. A., Getzoff, E. D., Beem, K. M., Richardson, J. S. & Richardson, D. C. (1982). *J. Mol. Biol.* **160**, 181–217.
Tainer, J. A., Getzoff, E. D., Richardson, J. S. & Richardson, D. C. (1983). *Nature (London)*, **306**, 284–287.
Than, M. E., Hof, P., Huber, R., Bourenkov, G. P., Bartunik, H. D., Buse, G. & Soulimane, T. (1997). *J. Mol. Biol.* **271**, 629–644.
Tullius, T. D., Frank, P. & Hodgson, K. O. (1978). *Proc. Natl Acad. Sci. USA*, **75**, 4069.
Wang, H., Bryant, C., Randall, D. W., LaCroix, L. B., Solomon, E. I., LeGros, M. & Cramer, S. P. (1998). *J. Phys. Chem.* B**102**, 8347.
Wang, X., Grush, M. M., Froeschner, A. G. & Cramer, S. P. (1997). *J. Synchrotron. Rad.* **4**, 236–242.
Watenpaugh, K. D., Sieker, L. C. & Jensen, L. H. (1980). *J. Mol. Biol.* **138**, 615.
Yang, Y., DuBois, J. L., Hedman, B., Hodgson, K. O. & Stack, T. D. P. (1998). *Science*, **279**, 537–540.
Zhang, H. H., Filipponi, A., DiCicco, A., Lee, S. C., Scott, M. J., Holm, R. H., Hedman, B. & Hodgson, K. O. (1996). *Inorg. Chem.* **35**, 4819–4828.
Zhang, H. H., Filipponi, A., DiCicco, A., Scott, M. J., Holm, R. H., Hedman, B. & Hodgson, K. O. (1997). *J. Am. Chem. Soc.* **119**, 2470–2478.
Zhu, Z., Cunane, L. M., Chen, Z. W. & Durley, R. C. W. (1999). Unpublished.